

## OPTIMIZED DESIGN OF STRAIN-COMPENSATED $\text{In}_x\text{Ga}_{1-x}\text{N}/\text{GaN}$ AND $\text{In}_x\text{Ga}_{1-x}\text{N}/\text{In}_y\text{Ga}_{1-y}\text{N}$ MULTIPLE-QUANTUM-WELL LASER DIODES

F. HADJAJ\*, M. BELHADJ, K. LAOUFI, A. MISSOUM

*Laboratory of semiconductor devices physics (LPDS), University of Bechar,  
P.O.BOX 417, Bechar 08000, Algeria*

We carried out a study of the strain-compensated  $\text{In}_x\text{Ga}_{1-x}\text{N}/\text{GaN}$  and  $\text{In}_x\text{Ga}_{1-x}\text{N}/\text{In}_y\text{Ga}_{1-y}\text{N}$  multiple quantum wells, In order to carry out this analysis, we choose a set of three different types of samples. The optimization of this laser structure allowed us to determine the optimal values of the functional parameters, in order to adjust their performance and interest. We also studied the electronic and structural properties of compound semiconductor alloys used in wurtzite phase and we have presented a comparative theoretical study of both structures. Our studies show the improvement of the spontaneous emission spectra and better carrier confinement from the use of  $\text{In}_x\text{Ga}_{1-x}\text{N}/\text{In}_y\text{Ga}_{1-y}\text{N}$  MQW with higher In-content in barrier as active regions for diode lasers and this structure is useful for the design of new high performance Laser diodes emitting in the Blue/Violet range, and it's also shows that the process of the electron-holes transition is strongly affected by the quantum well width and the Indium composition, and the InGaN lattice mismatch that increases with In-content causing the strain accumulation inside the QW structure. However, strain is undesirable as it can cause defects such as cracking at the interface. We can optimize the InGaN/GaN strained quantum well structures to achieve a reliable optoelectronic component. It suffices to incorporate small amounts of indium in the barrier enhances the annihilation of the defect and strain, thereby improving their structural properties.

(Received December 16, 2020; Accepted March 4, 2021)

*Keywords:* III-nitrides,  $\text{In}_x\text{Ga}_{1-x}\text{N}/\text{GaN}$ ,  $\text{In}_x\text{Ga}_{1-x}\text{N}/\text{In}_y\text{Ga}_{1-y}\text{N}$  Multiple Quantum Well laser

### 1. Introduction

The III-Nitride semiconductors have attracted much attention over recent years because of their potential applications in technological devices. This is due mainly to the fact that the energy gap can be tuned over a wide spectral range from the visible to the ultraviolet region of the electromagnetic spectrum. Although the zinc blende and wurtzite structures are present in the GaN, AlN, and InN semiconductors [1]. The vast majority of research on III-V nitrides has been focused on the wurtzite crystal phase. The reason is that sapphire substrates tend to transfer their hexagonal symmetry to the nitride films grown on them. As such, interest in zinc blende nitrides has been growing recently [2] the hexagonal wurtzite structure is extensively utilized because all the III-nitride semiconductors and their alloys exhibit a direct band gap energy, which results in a high emitting performance. Due to the remarkable progress in epitaxial growth technology, high quality samples of these compounds can be produced. III-Nitrides have recently attracted attention as a promising material class for high-power, high frequency microelectronic applications at elevated temperatures. They possess large band gaps, relatively small effective masses in the conduction band minimum, large offsets to the conduction band satellite valleys, and high polar optical phonon frequencies [3]. For nitride based ternary alloys, due to the smaller bandgap energy of InGaN material than that of GaN, InGaN ternary alloy can be used as a promising active heterostructure or QW material to emit in the violet and blue region of the spectrum with a carrier confinement layer of AlGaN. The In and Al content in each respective layer is commonly less than 20% when consider having a high quality film. In 1990, There has been significant process in the

---

\*Corresponding author: hadjadj.fatima@univ-bechar.dz

growth and characterization of the InGaN material [4]-[5]. The bandgap energy of InGaN measured by Osamura et al [6].

In this work, we present a comprehensive analysis of wavelength, transition energy, spontaneous emission and confinement factor for w-In<sub>x</sub>Ga<sub>1-x</sub>N/GaN and w-In<sub>x</sub>Ga<sub>1-x</sub>N/In<sub>y</sub>Ga<sub>1-y</sub>N multiple quantum well laser ( wurtzite (wz-) phase) emitting in the Blue/ Violet range (between 390 nm and 490 nm) and the two structure are compared.

## 2. Theoretical model and device structure

The quantum well is a single layer of one narrow band gap ( $E_g(QW)$ ) semiconductor which is sandwiched between two layers of a wider band gap material ( $E_g$  (barrier)), such as In<sub>x</sub>Ga<sub>1-x</sub>N as a well and GaN as a barrier, or from one material but with different mole fractions in the well and barrier, such as In<sub>x</sub>Ga<sub>1-x</sub>N as a well and In<sub>y</sub>Ga<sub>1-y</sub>N as a barrier where the condition  $E_g(Barrier) > E_g(QW)$  must be inquired. The active region of the laser structure consists of 3 nm-wide In<sub>0.2</sub>Ga<sub>0.8</sub>N QWs with 5 nm-wide GaN barriers and was embedded in a 0.4 μm wide Al<sub>0.12</sub>Ga<sub>0.88</sub>N cladding layers. We also grew a second laser sample, which contained a structure identical to the first sample, except for a barrier that has been changed to In<sub>y</sub>Ga<sub>y</sub>N which has In-content vary from 0.01 to 0.15 to match the desired emission wavelength chosen from the range of 390-490 nm. The MQWs active region consists of three nominally identical In<sub>0.2</sub>Ga<sub>0.8</sub>N wells each of them having a width of 3 nm and GaN, In<sub>0.01</sub>Ga<sub>0.99</sub>N or In<sub>0.15</sub>Ga<sub>0.85</sub>N barrier with a width of 5 nm, and were sandwiched between 0.4 μm Al<sub>0.12</sub>Ga<sub>0.88</sub>N cladding layers.

The design of a heterostructure (a key element of any optoelectronic devices) consists in assembling crystalline materials with different band gaps and refractive indices but with similar lattice constants in order to obtain a pseudomorphic growth [7]. In semiconductors, the band gap depends upon the temperature mainly due to the lattice expansion and the electron-lattice interaction. The Varshni formula describes well the temperature dependence of the band gap in nitrides. The temperature dependence of the band gap is calculated by:

$$E_g(T) = E_g(0) - \frac{\alpha \cdot T^2}{\beta + T} \quad (1)$$

where  $E_g(T)$  is the bandgap energy at temperature T,  $E_g(0)$  is the bandgap energy at 0 K,  $\alpha$  and  $\beta$  are material-related constants. The value of  $\beta$  is approximately equal to the Debye temperature at 0 K. [8],  $\alpha$  and  $\beta$  for GaN, InN and AlN are shown Table.1. Yet very dispersed values of  $\alpha$  and  $\beta$  are reported in the literature. The band gap of A<sub>x</sub>B<sub>1-x</sub>C is then interpolated by:

$$E_g^{A_xB_{1-x}C} = x \cdot E_g^{AC} + (1 - x) \cdot E_g^{BC} + b \cdot x \cdot (1 - x) \quad (2)$$

where  $E_g^{ABC}$  is the band gap of the alloys for a composition x.  $E_g^{AC}$  and  $E_g^{BC}$  are the band gap of the binary constituents AC and BC, respectively, where b is the bowing parameter specific to each compound and determined experimentally [9]. There is a large spread and uncertainty of values for bowing parameters in the literature. For example, the bowing parameter of 1.43 eV is often used in band calculations of InGaN. Meanwhile, a value of 1.3 eV for AlGaIn [10]. The refractive index value in nitrides as in other materials is very important to achieve a proper confinement of light in the active region of a semiconductor. Accurate refractive index values for InGaIn and AlGaIn materials are required to optimize the laser diode [11]. The refractive index of In<sub>x</sub>Ga<sub>1-x</sub>N and Al<sub>x</sub>Ga<sub>1-x</sub>N are calculated using an approximate method as follows:

$$n^{A_xB_{1-x}C} = x \cdot n^{AC} + (1 - x) \cdot n^{BC} = (n^{AC} - n^{BC}) \cdot x + n^{BC} \quad (3)$$

$n^{AC}$  and  $n^{BC}$  are the refractive indices of the materials, AC and BC, respectively. The refractive indices of InN, GaN and AlN are set as 3.4167, 2.5067, and 2.0767, respectively [12]. The

effective masses of electron and holes for ternary alloys used in our laser simulation were calculated using Eq. (4), and Eq. (5) below:

$$m_e^{A_xB_{1-x}C} = x \cdot m_e^{AC} + (1-x) \cdot m_e^{BC} = (m_e^{AC} - m_e^{BC}) \cdot x + m_e^{BC} \quad (4)$$

$$m_{hh}^{A_xB_{1-x}C} = x \cdot m_{hh}^{AC} + (1-x) \cdot m_{hh}^{BC} = (m_{hh}^{AC} - m_{hh}^{BC}) \cdot x + m_{hh}^{BC} \quad (5)$$

where  $m_e^{A_xB_{1-x}C}$ ,  $m_{hh}^{A_xB_{1-x}C}$  and  $m_{lh}^{A_xB_{1-x}C}$  are the effective mass of electrons, heavy and light holes in ternary alloy respectively,  $m_e^{AC}$ ,  $m_e^{BC}$ ,  $m_{hh}^{AC}$ ,  $m_{hh}^{BC}$ ,  $m_{lh}^{AC}$  and  $m_{lh}^{BC}$  are effective masses for electrons, heavy and light hole, respectively in binary alloy and  $m_0$  is the electron mass in free space [10]-[13]. The parameters used in calculations are listed in the tables.1. These values were taken from the literature, the values vary between sources due to different growth regimes and substrates being employed in each case. In some cases, data is not yet unavailable.

*Table 1. Band gap and effective masses values for WZ binary GaN, AlN, and InN alloys and their Varshni coefficients. Effective masses of the ternary alloys are calculated according to Vegard's.*

Compound	Parameters						
	$E_g(0 \text{ K})$ [eV]	$E_g(300 \text{ K})$ [eV]	$\alpha$ [MeV/K]	$\beta$ [K]	$m_e^*/m_0$	$m_{hh}^*/m_0$	$m_{lh}^*/m_0$
GaN	3.510 <sup>a</sup>	3.438 <sup>d</sup>	0.909 <sup>a</sup>	830 <sup>a</sup>	0.151 <sup>c</sup>	1.595 <sup>c</sup>	0.261 <sup>c</sup>
AlN	6.25 <sup>a</sup>	6.158 <sup>d</sup>	1.799 <sup>a</sup>	1462 <sup>a</sup>	0.48 <sup>b</sup>	3.53 <sup>b</sup>	3.53 <sup>b</sup>
InN	0.78 <sup>a</sup>	0.756 <sup>d</sup>	0.245 <sup>a</sup>	624 <sup>a</sup>	0.1 <sup>c</sup>	1.44 <sup>c</sup>	0.157 <sup>c</sup>

<sup>a</sup>Ref. [14], <sup>b</sup>Ref. [15], <sup>c</sup>Ref. [10], [16], <sup>d</sup>Ref. Calculated.

The energy levels available for both electrons and holes in a quantum well are quantized. Additionally, in quantum wells, for the direction perpendicular to the layers, we have the selection rule instead of momentum conservation, which states that only transitions between states of the same quantum number in the valence band and conduction band are allowed. Spacing between the energy levels for electrons and holes are different due to different effective mass of electron and hole [17]. Where  $E_{cn}$  and  $E_{vn}$  ( $n = 0, 1, 2, \dots$ ) are the quantized energy levels in conduction and valence band respectively.  $\Delta E_c$  and  $\Delta E_v$  are the discontinuities of the band edges of conduction and valence bands at the heterojunction, The band-offset ratio  $\Delta E_c/\Delta E_v$  of InGaN/GaN and InGaN/InGaN is assumed to be 0.7/0.3 and 7/3, respectively which are obtained from Ref.[18]-[19]. Quantized energy levels in the valence band are calculated by the same process. Using the parabolic band model  $E_{cn}$  be obtained by solving the eigenvalue equations:

$$\frac{m_{cb}}{m_{cw}} = \sqrt{\frac{\Delta E_c - E_{cn}}{E_{cn}}} \begin{cases} \tan \\ -\cot \end{cases} \left[ \frac{W \cdot \sqrt{2 \cdot m_{cw} \cdot E_{cn}}}{2 \cdot \hbar} \right] \begin{cases} \{n: \text{even}\} \\ \{n: \text{odd}\} \end{cases} \quad (6)$$

where  $\hbar = h/2 \cdot \pi$  is Plank's constant,  $W$  is the well width, and  $m_{cw}$  and  $m_{cb}$  are the effective masses of electrons inside of the well, and the barrier, respectively, In the range  $E_{cn} \ll \Delta E_c$ ,  $\Delta E_v$  can be shown to be approximated as:

$$E_{cn} = \frac{\left[ \frac{(n+1) \cdot \pi}{2} \cdot \frac{a_c}{W + \Delta W_c} \right]^2}{1 + \left\{ \frac{(n+1) \cdot \pi}{2} \right\}^2 \cdot b_c \cdot \left( \frac{\Delta W}{W + \Delta W_c} \right)^3} \quad (7)$$

with  $\Delta W_c = \frac{a_c}{\sqrt{b_c \cdot \Delta E_c}}$

$$\text{where } a_c = \frac{2\hbar}{\sqrt{2m_{cw}}}, \quad b_c = \frac{m_{cw}}{m_{cb}}$$

The wavelength corresponding to the transition between a conduction electron and a heavy hole at each subband edge is given by:

$$\lambda_n = 1.24/[E_g + E_{cn} + E_{vn}](\mu\text{m}) \quad (8)$$

The transition energy,  $E_{tr}$  between the quantized energy levels is given by [19]-[20]:

$$E_{tr} = E_g + E_{cn} + E_{vn} \quad (9)$$

Where  $v = hh$  or  $lh$  is an index for  $hh$  or  $lh$  subbands, respectively.

### 3. Simulation results and discussion

The realization of ternary compounds such as  $\text{In}_x\text{Ga}_{1-x}\text{N}$  and  $\text{Al}_x\text{Ga}_{1-x}\text{N}$  offers numerous solutions for the fabrication of electronic and optoelectronic components. Indeed, these materials have a wide band gap between two extremes corresponding to the gaps of the binary semiconductors used. The energy of the band gap varies depending on the composition of the materials and the temperature. The Fig.1 illustrates the behavior of the band gap energy and the corresponding emission wavelength of ternary  $\text{In}_x\text{Ga}_{1-x}\text{N}$  alloys as a function of Indium for the wurtzite structures.

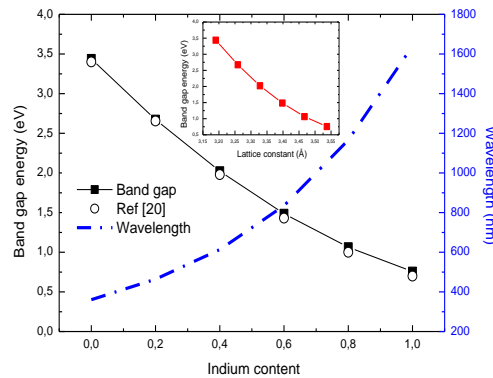


Fig.1. Band gap energy and the corresponding emission wavelength as a function of In-content ( $x$ ) for wurtzite  $\text{In}_x\text{Ga}_{1-x}\text{N}$  alloys at 300 K. The indium content is ranged from 0 (GaN) to 1 (InN), the open circles are the calculated values of the band gap obtained by N. Akter et al [21] for comparison.

The band gap energy reduces as the In-content increases from 3.438 to 0.756, while the emission wavelength of the  $\text{In}_x\text{Ga}_{1-x}\text{N}$  alloy covers the regime from 360.7 nm up to 1640 nm. By increasing the Indium content, the gap decreases until it reaches the gap of InN. The broad wavelength coverage indicates the accessibility of the  $\text{In}_x\text{Ga}_{1-x}\text{N}$  alloy to the Blue /Violet spectral regime (390 nm-490 nm). The emission wavelength is determined by the band gap 3.438 eV for GaN and 0.756 eV for InN, and the emission of ternary alloys  $\text{In}_x\text{Ga}_{1-x}\text{N}$  lies within this range. Our results are in good agreement with data of references [21]. The inset shows the band gap energy as function of the lattice constant. Addition of Indium to GaN has the effect of increasing the lattice constant whilst decreasing the band-gap.

The two GaN and InGaN layers that form the  $\text{In}_x\text{Ga}_{1-x}\text{N}/\text{GaN}$  quantum well heterostructure are different in their lattice parameters  $a$  and  $c$ , so there is a strain at the interface due to the lattice mismatch between the quantum well and the barrier. In fig.2, we show the variation of the  $\Delta a/a$  and  $\Delta c/c$  lattice mismatch of the quantum well  $\text{In}_x\text{Ga}_{1-x}\text{N}/\text{GaN}$  as a function of Indium content.

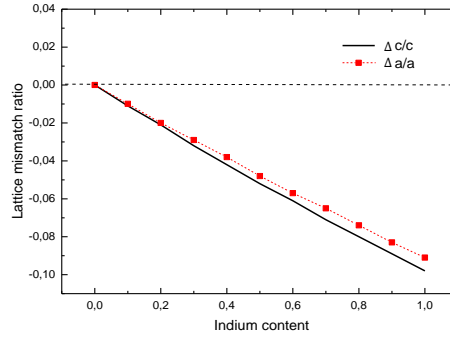


Fig.2. Lattice mismatch ratio of  $\text{In}_x\text{Ga}_{1-x}\text{N}/\text{GaN}$  along  $c$ -axis and  $a$ -axis as a function of the Indium content.

As shown in Fig.2, the lattice mismatch increases with the increase in the Indium content,  $x$ . It is in fact a compressive strain at the interface of  $\text{In}_x\text{Ga}_{1-x}\text{N}/\text{GaN}$ . It is observed that the lattice mismatch is negative ( $\Delta a/a < 0$  and  $\Delta c/c < 0$ ), whatever the value of the Indium content. From the results, we can see that our structure is compressive because the biaxial strain is negative; the lattice constant of the  $\text{In}_x\text{Ga}_{1-x}\text{N}$  well ( $a \sim 3.259 \text{ \AA}$  for  $x = 0.2$ ) is greater than that of the GaN barrier whose lattice constant is  $5.1896 \text{ \AA}$ . From the lattice constant of GaN and InN binary compounds, it is possible to determine the lattice constant of InGaN using Vegard's law. The  $a$ -lattice constants were determined as  $3.1896 \text{ \AA}$  and  $3.5365 \text{ \AA}$  for GaN and InN, respectively while the  $c$ -lattice constants are  $5.1855 \text{ \AA}$  and  $5.7039 \text{ \AA}$  for GaN and InN, respectively. When we apply concentrations of Indium equal to 0.2, compared with GaN barrier, the  $\text{In}_y\text{Ga}_{1-y}\text{N}$  barrier exhibits a smaller lattice mismatch along both the  $a$ - and  $c$ -axes with  $\text{In}_x\text{Ga}_{1-x}\text{N}$  well. The lattice mismatches between  $\text{In}_{0.2}\text{Ga}_{0.8}\text{N}$  and GaN are  $-2.1 \%$  ( $a$ -axis) and  $-2 \%$  ( $c$ -axis). The strains in  $\text{In}_{0.2}\text{Ga}_{0.8}\text{N}$  on  $\text{In}_{0.01}\text{Ga}_{0.99}\text{N}$  were found to be  $-2 \%$  ( $a$ -axis),  $-1.9 \%$  ( $c$ -axis) and strain along the  $a$ -axis ( $-0.53 \%$ ) and  $c$ -axis ( $-0.49 \%$ ) in  $\text{In}_{0.2}\text{Ga}_{0.8}\text{N}$  on  $\text{In}_{0.15}\text{Ga}_{0.85}\text{N}$ . The lattice mismatch allows the generation of dislocation defects at the interface of the heterostructure. Thus, reducing mismatch helps reduce structural defects in the interface. The  $\text{In}_x\text{Ga}_{1-x}\text{N}/\text{In}_y\text{Ga}_{1-y}\text{N}$  structure could be used to build quantum wells (QWs) with good structural qualities.

The Spontaneous emission spectra curves (TE mode) for 3nm  $\text{In}_{0.2}\text{Ga}_{0.8}\text{N}/\text{GaN}$  QW with various carrier density are calculated as shown in Fig. 3(a). We can clearly see a blue-shift of the spontaneous emission's peak in the interval that goes from 2.6 to 3.2 eV because of the shrinkage of the bandgap. In addition, more the carrier injection becomes larger, more the peak emission increases significantly and shifted to shorter wavelength.

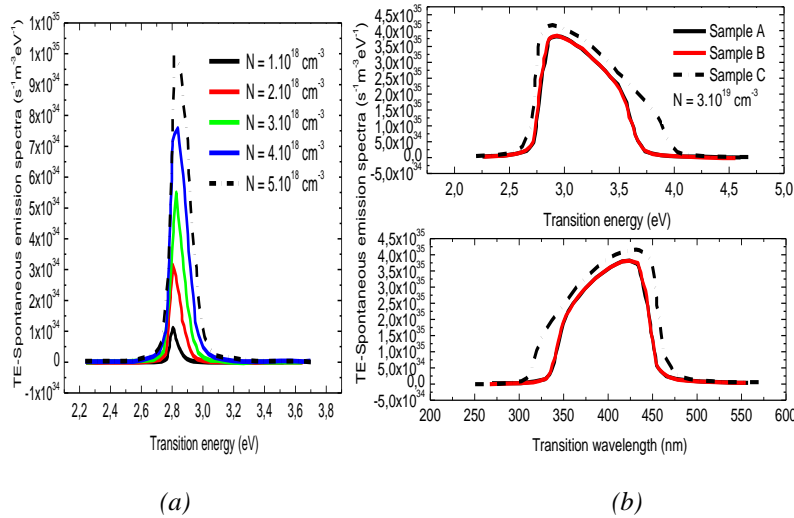


Fig. 3. (a) TE-Spontaneous emission spectra for strained  $\text{In}_{0.2}\text{Ga}_{0.8}\text{N}/\text{GaN}$  (sample A), SQWs structures with injected carrier density from  $1 \times 10^{18} \text{ cm}^{-3}$  up to  $5 \times 10^{18} \text{ cm}^{-3}$ ; (b) Spontaneous emission spectra for strained  $\text{In}_{0.2}\text{Ga}_{0.8}\text{N}/\text{GaN}$  (sample A),  $\text{In}_{0.2}\text{Ga}_{0.8}\text{N}/\text{In}_{0.01}\text{Ga}_{0.99}\text{N}$  (sample B) and  $\text{In}_{0.2}\text{Ga}_{0.8}\text{N}/\text{In}_{0.15}\text{Ga}_{0.85}\text{N}$  (sample C) SQWs structures at injected carrier density of  $3 \times 10^{19} \text{ cm}^{-3}$ . The same value of intraband relaxation time (0.1 ps) is used in both calculations.

Fig. 3(b) illustrates the variation of the spontaneous emission spectra for the TE polarization as a function of transition energy and corresponding wavelength in the three samples for a carrier density of  $3 \times 10^{19} \text{ cm}^{-3}$  and intraband relaxation time  $\sim 0.1 \text{ ps}$  at a well width of 3 nm (5 nm barrier widths) and at room temperature, Note that the three structures have the same parameters for comparison purpose. It is noted that the spontaneous emission spectra for both cases have only one peak which corresponds to e1-hh1 transition.  $\text{In}_{0.2}\text{Ga}_{0.8}\text{N}/\text{In}_{0.15}\text{Ga}_{0.85}\text{N}$  QW structure has much larger spontaneous emission than the other samples studied, this later which are similar and this is due to the close ratio of indium to each of them. As indicated in Fig.3 (b), the spontaneous emission, for  $\text{In}_{0.2}\text{Ga}_{0.8}\text{N}/\text{In}_{0.15}\text{Ga}_{0.85}\text{N}$  QW (sample C) shows a significant enhancement over that of the  $\text{In}_{0.2}\text{Ga}_{0.8}\text{N}/\text{GaN}$  QW (sample A). However, both QW structures  $\text{In}_{0.2}\text{Ga}_{0.8}\text{N}/\text{GaN}$  and  $\text{In}_{0.2}\text{Ga}_{0.8}\text{N}/\text{In}_y\text{Ga}_{1-y}\text{N}$  with lower In-content (1 %) exhibit lower spontaneous emission in comparison to those of higher In-contents (15 %). the spontaneous emission's peak for sample A is found at the transition energy  $\sim 2.887 \text{ eV}$ , and at corresponding lasing wavelength  $\sim 430 \text{ nm}$ ; while in sample C the spontaneous emission's peak is found at photonic energy  $\sim 2.835 \text{ eV}$  and at corresponding wavelength  $\sim 438 \text{ nm}$ . By increasing the In-content, it is possible to extend the emission of InGaN-based lasers to longer wavelengths.

The width of the quantum well and the composition  $x$  have an important influence on the transition process in the well whether it is the transitions between electrons of the first level e1 with the holes of the level hh1 or with those of the level lh1. In Fig. 4 (a), we have plotted the calculated transition wavelength for the first ( $1^{\text{st}}$ :  $n=0$ ) and second ( $2^{\text{nd}}$ :  $n=1$ ) transitions between both electrons and heavy holes levels, electrons and light holes levels as a function of the well width for the  $\text{In}_{0.2}\text{Ga}_{0.8}\text{N}/\text{GaN}$  QW structure, the width of the barriers is kept constant at 5 nm.

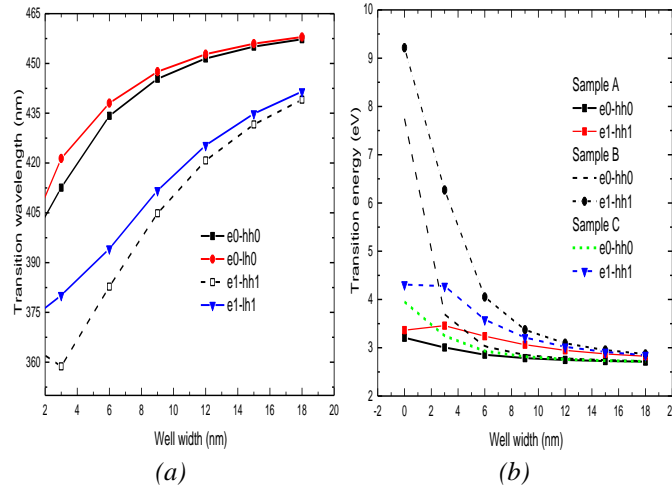


Fig.4. Transition wavelength corresponding to the first ( $1^{\text{st}}$ ) and second ( $2^{\text{nd}}$ ) transitions between the quantized energy levels of (a) conduction electrons and heavy holes and conduction electrons and light holes as a function of the well width of strained  $\text{In}_{0.2}\text{Ga}_{0.8}\text{N}/\text{GaN}$  (sample A) QW structures at room temperature, (b) conduction electrons and heavy holes as a function of the well width of strained  $\text{In}_{0.2}\text{Ga}_{0.8}\text{N}/\text{GaN}$  (sample A),  $\text{In}_{0.2}\text{Ga}_{0.8}\text{N}/\text{In}_{0.01}\text{Ga}_{0.99}\text{N}$  (sample B) and  $\text{In}_{0.2}\text{Ga}_{0.8}\text{N}/\text{In}_{0.15}\text{Ga}_{0.85}\text{N}$  (sample C) SQWs structures at room temperature.

Following the curves presented in this figure, we see that the transition wavelength of the QW structure increases rapidly as the width of the  $\text{In}_x\text{Ga}_{1-x}\text{N}$  QW increases. We can also see that for the light holes, the well width effect is more marked as compared to the heavy holes. The accessible domain of emission of the  $\text{In}_{0.2}\text{Ga}_{0.8}\text{N}/\text{GaN}$  quantum well structure for the second two energy levels ( $n=1$ ) occurred between the conduction band and the heavy holes band and the conduction band and the light holes band extends in  $\lambda = 384 \text{ nm}$  to  $444.8 \text{ nm}$  for well width between 1 nm and 20 nm, that is to say it covers a large range of emission in the visible spectrum from violet to blue.

The variation of the transition energies  $E_{tr}$  (e-hh) as a function of the well width in the three samples studied is illustrated in Fig.4(b). We notice that the transition energies decrease with the increase in the width of the well. This reduction is interpreted by the decrease in quantization energies which automatically implies the increase in wavelength. For high widths, we observed that the behavior of the electronic interband transitions in  $\text{In}_{0.2}\text{Ga}_{0.8}\text{N}/\text{GaN}$  is similar to the shown for  $\text{In}_{0.2}\text{Ga}_{0.8}\text{N}/\text{In}_{0.01}\text{Ga}_{0.99}\text{N}$  and  $\text{In}_{0.2}\text{Ga}_{0.8}\text{N}/\text{In}_{0.15}\text{Ga}_{0.85}\text{N}$  and we can also note that the  $\text{In}_{0.2}\text{Ga}_{0.8}\text{N}/\text{In}_{0.01}\text{Ga}_{0.99}\text{N}$  structure shows stronger transitions for the e0-hh0 and e1-hh1 as compared to those of the  $\text{In}_{0.2}\text{Ga}_{0.8}\text{N}/\text{In}_{0.15}\text{Ga}_{0.85}\text{N}$  QW structure.

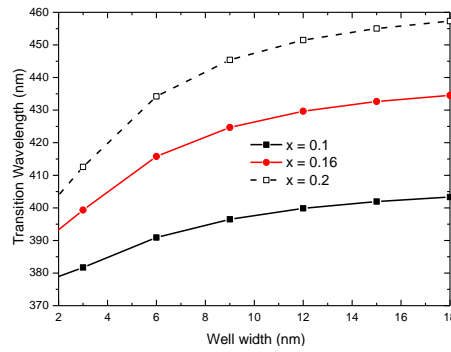


Fig. 5. Transition wavelength corresponding to the first ( $1^{st}$ ) transitions between the quantized energy levels of conduction electrons and heavy holes as a function of the well width of strained  $\text{In}_x\text{Ga}_{1-x}\text{N}/\text{GaN}$  QW structures with several Indium content.

The transition wavelength between the  $n = 0$  electron level and the  $n = 0$  heavy-hole level as a function of QW width for single QWs for indium content  $x = 0.2$  are shown in Fig.5. The emission wavelength increases toward longer wavelengths with increasing QW width, but its rate of increase was reduced for smaller Indium content. Similar results were obtained by Park, et al [22], using a similar structure crystallize in the zinc blende instead of the wurtzite.

We plot in Fig.6 the confinement factor as a function of the width of the active zone for the three quantum well structures. The calculations are carried out for a wavelength  $\lambda = 430$  nm for sample A and B and  $\lambda = 438$  nm for sample C. Note that the confinement factor increases with the width of the well. The well enlargement improves the confinement factor of our laser structures.

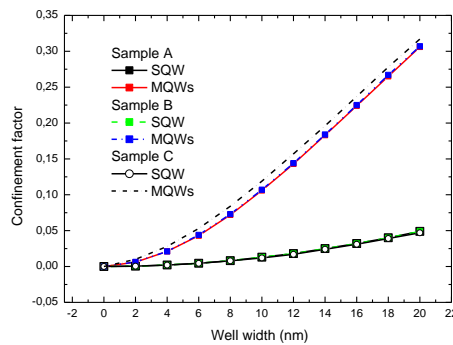


Fig.6. The confinement factor as a function of the width of the well for strained  $\text{In}_{0.2}\text{Ga}_{0.8}\text{N}/\text{GaN}$  (sample A),  $\text{In}_{0.2}\text{Ga}_{0.8}\text{N}/\text{In}_{0.01}\text{Ga}_{0.99}\text{N}$  (sample B) and  $\text{In}_{0.2}\text{Ga}_{0.8}\text{N}/\text{In}_{0.15}\text{Ga}_{0.85}\text{N}$  (sample C) SQWs structures at room temperature.

The results obtained in the case of a multi-well structure (MQW) are significantly greater than those obtained by using a single-well structure (SQW) such increase in the refractive index of the lateral layers, which provides good confinement of light in the active layer, so, the factor confinement is improved when we replace the single well with a multi quantum well (MQW) structure. This figure illustrates also that the confinement factor for the  $\text{In}_{0.2}\text{Ga}_{0.8}\text{N}$  QWs with GaN

barriers decrease over the  $\text{In}_{0.2}\text{Ga}_{0.8}\text{N}/\text{In}_{0.15}\text{Ga}_{0.85}\text{N}$  QW. The higher In-content in the barrier provides better carrier confinement in the  $\text{In}_x\text{Ga}_{1-x}\text{N}/\text{In}_y\text{Ga}_{1-y}\text{N}$  QWs. It can be seen that  $\Gamma$  increases with width of well and Indium content. We also notice that the confinement for  $\text{In}_{0.2}\text{Ga}_{0.8}\text{N}/\text{GaN}$  QWs having three quantum wells,  $\Gamma = 0.012$  which means that this factor has been multiplied by three,  $\Gamma = 0.001$  for the single-well, and that for a width of 3 nm. The confinement factors of  $\text{In}_{0.2}\text{Ga}_{0.8}\text{N}/\text{GaN}$  (samples A) and  $\text{In}_{0.2}\text{Ga}_{0.8}\text{N}/\text{In}_{0.01}\text{Ga}_{0.99}\text{N}$  (sample B) are almost the same. Finally, the increase in the strain in structure (as in the case of sample A) also caused a slight decrease in confinement factor.

#### 4. Conclusion

In summary, we have introduced our work on wurtzite III-nitrides, mainly on the results of Wz-InGaN, Wz-InGaN/GaN and Wz-InGaN/InGaN quantum wells structures. The focus of this work has been on the achievement of high quality quantum wells and the investigation of the structural and optical properties of Wz-InGaN. We observe that the introduction of indium content decreases the band gap energy and therefore the energy of the various interband transitions in the well and this opens the possibility to achieve longer wavelength emission. We see also that the wavelengths increase with the width of the well. This increase begins as linear and there after it becomes constant. The lattice constant of InGaN is larger than that of the GaN, which induce the compressive strain in the QW. Moreover, as In-content increases, the lattice-mismatch induces increased strain of interface InGaN /GaN which leads to cause a variety of defects to the materials.

Therefore, one can see that the low In-content in ternary  $\text{In}_x\text{Ga}_{1-x}\text{N}$  alloy is widely used as an active layer to fabricate high-brightness Laser diodes. On the other hand, we also show that an enhancement of the spontaneous emission and confinement factor was achieved for QWs emitting in blue and violet spectral regimes. A more significant increase in the efficiency was observed in the case of barrier with higher indium content QWs (or compressive strain barrier). The  $\text{In}_x\text{Ga}_{1-x}\text{N}/\text{In}_y\text{Ga}_{1-y}\text{N}$  quantum well Lasers with higher In-content have demonstrated a improved laser performance with regard to  $\text{In}_x\text{Ga}_{1-x}\text{N}/\text{GaN}$  lasers, so, it is important to emphasize that the uses of InGaN barriers with higher indium content exhibit improved spontaneous spectra and confinement over that of the structure with lower In-content which means that the incorporation Indium into the barrier of  $\text{In}_x\text{Ga}_{1-x}\text{N}/\text{GaN}$  lasers can reduce the overall compressive strain, which provides benefits for material growth and thus leading to improve optical efficiency and laser performance. Finally, our study suggests that the barrier  $\text{In}_y\text{Ga}_{1-y}\text{N}$  with higher indium content is the optimal candidate for InGaN-based QWs.

#### References

- [1] E. R. Murthy, A. Srivani, G. Raghavaiah, *Int. J. Thin. Fil. Sci. Tec.* **6**(1), 15 (2017).
- [2] S. Berrah, H. Abid, A. Boukortt, M. Sehil, *Turk J Phys* **30**, 513 (2006).
- [3] V. R. Murthy, A. Srivani, G. V. Raghavaiah, *Int. J. Thin. Fil. Sci. Tec.* **6**(1), 15 (2017).
- [4] S. Nakamura, M. Senoh, T. Mukai, *Appl. Phys. Lett.* **62**, 2390 (1993).
- [5] S. Nakamura, M. Senoh, N. Iwasa, S. Nagahama, *Appl. Phys. Lett.* **67**, 1868 (1995).
- [6] K. Osamura, K. Nakajima, Y. Murakami, *Solid State Commun.* **11**, 617 (1972).
- [7] B. Gil, O. Briot, *Phys. Rev. B* **55**, 2530 (1997).
- [8] Y. P. Varshini, *Physica Status Solidi* **34**(1), 149 (1967).
- [9] M. D. McCluskey, C. G. Van de Wall, C. P. Master, L. T. Romano, N. M. Johnson, *Applied Physics Letters* **72**(21), 1998.
- [10] A. Z. Goharrizi, F. Z. Jasim, Z. Hassan, K. Omar, H. A. Hassan, *International Journal of the Physical Sciences* **7**(4), 566 (2012).
- [11] E. Rosencher, B. Vinter, *Optoelectronics*, Cambridge University Press, Cambridge, 2002.
- [12] W. Wang, W. Xie, Z. Deng, M. Liao, *Micromachines* **10**, 875 (2019).
- [13] M. I. Ahamed, K. S. Kumar, E. E. Anand, A. Sivaranjani, *Journal of Ovonic Research* **16** (4), 245 (2020).

- [14] I. Vurgaftman, J. R. Meyer, Journal of applied physics **94**, 3675 (2003).
- [15] NSM Archive. Physical Properties of Semiconductors. IOFFE Physical Technical Institute. 2013.
- [16] S. M. Thahab, H. Abu Hassan, Z. Hassan, Chinese Optics Letters **7**(3), 2009.
- [17] D. A. B. Miller, Quantum Dynamics of Simple Systems: Proceedings of the Forty Fourth Scottish Universities Summer School in Physics, Stirling, August 1994. Institute of Physics, London, 1996.
- [18] J. Piprek, S. Nakamura, IEE Proc.-Optoelectron. **149**(4), 2002.
- [19] B.T. Liou, S. H. Yen, C.Y. Lin, Y. K. Kuo, Hsiuping Journal **13**, 297 (2006).
- [20] K.Fellaoui, D.Abouelaoualim, A.Elkadadra, A.Oueriagli, Journal of Nano-and Electronic Physics **7**(4), 04061 (2015).
- [21] N. Akter, International Journal of Research in Engineering and Technology (IJRET) **3**(1), 315 (2014).
- [22] S. H. Park, Y. T. Lee, Chin Phys Lett. **27**(4), 044208 (2010).